Siva Darbha was born in Ottawa, ON and attended the University of Toronto, where he majored in engineering science. During his undergraduate career, he held an internship at the European Organization for Nuclear Research in the summer of 2006, and a SULI internship at the Stanford Linear Accelerator Center in the summer of 2007. He seeks to enter a PhD program in nuclear science and engineering and to conduct research at a national laboratory. His interests include literature, film, and graphic novels.

Lewis Keller is an engineering physicist at the Stanford Linear Accelerator Center (SLAC). He received a B.S. degree from Valparaiso University and a Ph.D. from Oklahoma State University in 1969. Following a post-doc appointment at Argonne National Laboratory, he joined SLAC as head of the Experimental Facilities Department in 1973. He collaborated on numerous fixed target and colliding beam experiments, and participated in the design of the Stanford Linear Collider and the BaBar Detector at PEP-II. He is currently working on design of the International Linear Collider and the LHC Accelerator Research Project.

Takashi Maruyama is a staff physicist at the Stanford Linear Accelerator Center. He received his Ph. D. in high energy physics from Tohoku University, Japan. His research interests include high energy e+e- interactions, particle tracking and radiation shielding, and polarized electron source based on semiconductor photocathodes.

Simulation of Neutron Backgrounds from the ILC Extraction Line Beam Dump

Siva Darbha, Lewis Keller, and Takashi Maruyama

ABSTRACT

The operation of the International Linear Collider (ILC) as a precision measurement machine is dependent upon the quality of the charge-coupled device (CCD) silicon vertex detector. An integrated flux of 10^{10} neutrons/cm^2 incident upon the vertex detector will degrade its performance by causing displacement damage in the silicon. One source of the neutron background arises from the dumping of the spent electron and positron beams into the extraction line beam dumps. The Monte Carlo program FLUKA was used to simulate the collision of the electron beam with the dump and to determine the resulting neutron flux at the interaction point (IP). A collimator and tunnel were added and their effect on the flux was analyzed. A neutron source was then generated and directed along the extraction line towards a model of the vertex detector to determine the neutron flux in its silicon layers. Models of the beampipe and BeamCal, a silicon-tungsten electromagnetic calorimeter in the very forward region of the detector, were placed in the extraction line and their effects on scattering were studied. The IP fluence was determined to be 3.7×10^{10} +/- 2.3×10^{10} neutrons/cm^2/year when the tunnel and collimator were in place, with no appreciable increase in statistics when the tunnel was removed. The BeamCal was discovered to act as a collimator by significantly impeding the flow of neutrons towards the detector. The majority of damage done to the first layer of the detector was found to come from neutrons with a direct line of sight from the first extraction line quadrupole QDEX1, with only a small fraction scattering off of the beampipe and into the detector. The 1 MeV equivalent neutron fluence was determined to be 9.3×10^{8} neutrons/cm^2/year from the electron beam alone. The two beams collectively contribute double to this fluence, which is 19% of the threshold value in one year. Future work will improve the detector model and other sources of neutron backgrounds will be analyzed.

Introduction

The Large Hadron Collider (LHC) operating at CERN will probe a new energy scale using 14 TeV center of mass energy proton-proton collisions and will produce a wealth of new physics, including searches for the Higgs boson and Supersymmetry [1]. The International Linear Collider (ILC) is a proposed linear electron-positron collider that will be 31 km in length and will have a center of mass energy of 500 GeV. It will have a cleaner signal to noise ratio than the LHC and will provide precision measurements for some of the physics discovered there.

The electron and positron beams in the ILC will have 2×10^{10} particles per bunch and a bunch separation of 370 ns with 2,625 bunches in 1 ms trains at a repetition rate of 5 Hz. The bunches will collide at the interaction point (IP) at a 14 mrad crossing angle [2]. The Beam Delivery System (BDS) in the ILC is responsible for transporting the electron and positron beams from the main linacs, colliding them at the IP, and discarding the spent beams to the extraction line beam dumps [Figure 1]. The beam dumps are stainless steel cylindrical containers of 75 cm radius and 7.5 m length with a titanium window of 15 cm radius and 1 mm thickness through which the beams enter. The dumps contain water at a pressure of 10 bar [3]. Water's high specific heat capacity makes it ideal to dissipate the energy of the beams. Only a minute fraction of the particles in any bunch crossing will interact, leaving on the order of 10^{14} high energy electrons and positrons to be extracted from the IP and discarded in the water dumps each second. The

dumps are designed to absorb 17 MW of beam power at a 500 GeV center of mass energy [3].

The extracted beams will interact with the H_2O molecules in the dump, leading to electromagnetic showers in which the resulting photons will produce a flux of neutrons through photonuclear interactions. The shower maximum, the locus of neutron production, occurs roughly 2 m into the water dump [4]. Though the majority of this 'gas' of neutrons will be forward directed, some will be backward directed and will reach the detector, a phenomenon called neutron backshine. The backshine creates unwanted backgrounds in the tracking devices and calorimeters that will obscure the physics processes observed from collision of the beams and may even cause displacement damage in the silicon atoms in the charge-coupled device (CCD) vertex detector if the integrated flux reaches a level higher than 10^{10} neutrons/cm^2, leading to charge traps [5, 6]. The accumulation of charge traps would degrade the performance of the detector by reducing the charge transfer along the CCD and by causing junction leakage [5, 6]. The CCD vertex detector is the innermost tracking system in the SiD detector model, one of the four detector models under consideration for the ILC. Such degradation would hinder the performance of the ILC as a precision machine and would require frequent repairs, which should be minimized to allow continuous and robust recording of data.

This paper investigates the neutron detector backgrounds from the extraction line beam dump through Monte Carlo simulations. The program FLUKA was used for the simulations due to its robustness with low energy neutron cross sections. Only the electron beam was used for the analysis, with the positron beam having symmetric and analogous results. The neutron fluxes at the dump and at the detector were studied first without material near the beam line to provide a benchmark estimate. Concrete tunnel walls and a concrete collimator were then added to the simulation and their effect on the flux was studied. Information gathered on neutron distributions at the dump during this work was used to simulate an isotropic and uniformly distributed neutron source. The source was positioned in the bore of the extraction line quadrupole QDEX1 and incident upon the beryllium beampipe and the five layers of the CCD silicon vertex detector central barrel to obtain an estimate of the neutron flux at the vertex detector. These values were integrated over a year into annual fluences. Particle biasing techniques were used to increase statistics on the simulated events, and the effectiveness of each bias was studied.

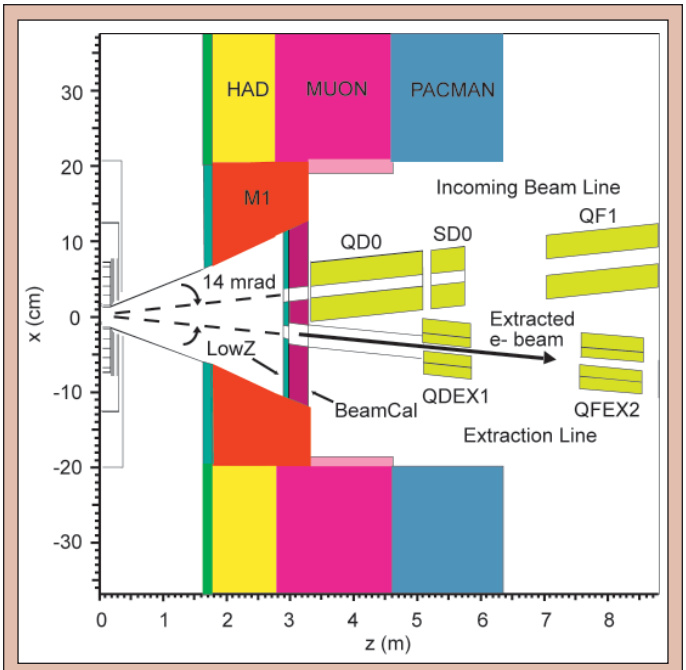

Figure 1. A Geant4 model of the extraction line. M1 is an instrument mask, HAD is the endcap hadronic calorimeter, MUON is the endcap muon calorimeter, and PACMAN is a beamline shielding ring to provide radiation shielding to the endcap detectors. In the incoming beam line, QD0 and QF1 are the final doublet quadrupole magnets and SD0 is the final sextupole. QDEX1 and QFEX2 are the first doublet quadrupoles in the extraction line. The water dump is located 300 m down the extraction line.

Materials and Methods

The Monte Carlo program FLUKA was used for the simulations. The spent electron beam was given an initial position at the origin and was directed in the positive z-direction with 250 GeV of energy. The beam was directed into the water dump, which was placed at z = 300 m and was modeled by a circular cylinder of water with a radius of 75 cm and a length of 5 m (see Figure 2). The stainless steel container and Ti window were ignored since they would not impede an outward flux of neutrons from inside the dump and would increase the computation time.

Although the ILC will have on the order of 10^{14} electrons incident on the water dump per second, only between 10^3 and 10^7 electrons can be simulated in FLUKA per run to maintain reasonable computation times. Performing subsequent runs to increase the statistics would be ineffective, for that approach would provide

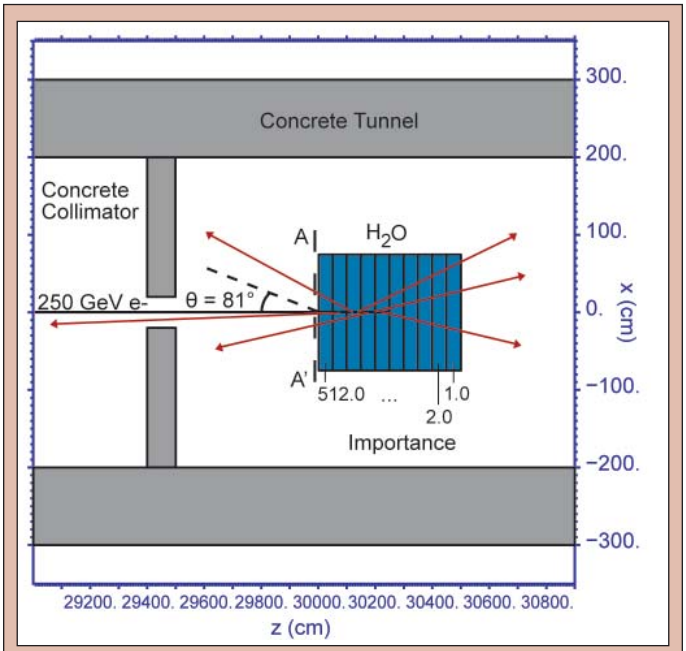

Figure 2. The FLUKA model of the beam dump with a concrete collimator and concrete tunnel in place. The 250 GeV input electron beam acts as a line source in the water dump, and the red arrows symbolize possible trajectories of the neutrons produced in the dump along that source.

an unnecessary level of precision at too great of a computation time. As a result, three particle biasing techniques were used to shift computation time towards simulating interesting events at the expense of uninteresting ones, effectively increasing the statistics on the fluence scoring by using computation time effectively and providing sufficient precision. First, leading particle biasing was activated for electrons, positrons, and photons with energy below 2.5 GeV. Since simulating a full electromagnetic shower requires long computation time, leading particle biasing traces only the most energetic secondary created by the electrons, positrons, or photons below 2.5 GeV and eliminates all others, adjusting the 'weight' of the most energetic particle accordingly. Secondly, the interaction cross section for neutron production by photonuclear interactions was increased by a factor of 50, and the 'weight' associated with each neutron produced this way was decreased by a factor of 50 to preserve particle multiplicity. Finally, the cylindrical water dump was divided into 10 adjacent regions as in Figure 3. The region at the back of the dump was given an 'importance' of 1.0, and each region progressively closer to z = 0 was given a factor of 2.0 larger importance. Photons crossing a region boundary from lower importance to higher importance were reloaded onto the particle transport stack an integer number of times, such that on average 2.0 photons exited the boundary for every one that entered; this sampling is called splitting. FLUKA adjusted the 'weight' associated with the new photons on the stack to conserve particle multiplicity when the bias was applied. The increase in photon multiplicity exacerbated the electromagnetic showering and increased neutron production through photonuclear interactions. Photons crossing a region boundary in the opposite direction were terminated similarly, a sampling called Russian Roulette [7]. The application of splitting and Russian Roulette focused the computation time on increasing statistics on backward directed neutrons at the expense of ignoring forward directed one, which do not contribute to backshine. The effectiveness of each type of bias was studied with 6,000 incident electrons (see Table 1).

Production and transport cutoffs were activated to decrease simulation time. A 50 MeV cutoff on both was applied to electrons and positrons, and a 10 keV cutoff on both was applied to photons. A transport cutoff of 1.0332×10^{-5} GeV was applied to neutrons. This value was chosen from Non-Ionizing Energy Loss (NIEL) scaling studies which show that neutrons below 10 keV do not have sufficient energy to create displacement damage, which are mostly from point defects and defect clusters, in the silicon bulk of the vertex detector [8]. The NIEL stopping power for neutrons in silicon also decreases with decreasing kinetic energy, and consequently neutrons below 10 keV were not a concern [9].

The neutron fluence decays exponentially as a function of cos θ for neutrons leaving the water dump in the negative z-direction, where θ is the zenith angle with respect to the z-axis. The distribution was measured on the surface of the dump at A-A' in Figure 2 and was partitioned into bins covering small ranges of cos θ, over each of which the fluence can be viewed as isotropic (see Figure 3) [10]. The fluence was assumed to be isotropic in the first bin, which corresponds to the range $-1 < \cos\theta < -0.99$ and an 8.1° spread around the negative z-direction from the surface of the water dump. This spread was sufficiently large that the expected scattering from the tunnel walls would be observed.

The relevant fluence value was that measured in a circle of 1.5 cm radius at z = 0, concentric with the z-axis and parallel to the xy-plane, which is the IP fluence. The neutrons that reach this circle are the ones that will reach the vertex detector, since they have passed through the bore of the first extraction line quadrupole, which has a radius of 1.5 cm and have not been impeded by collimators, magnets, or the tunnel. However, when a scoring plane that size was used, small fluence values with large errors were measured.

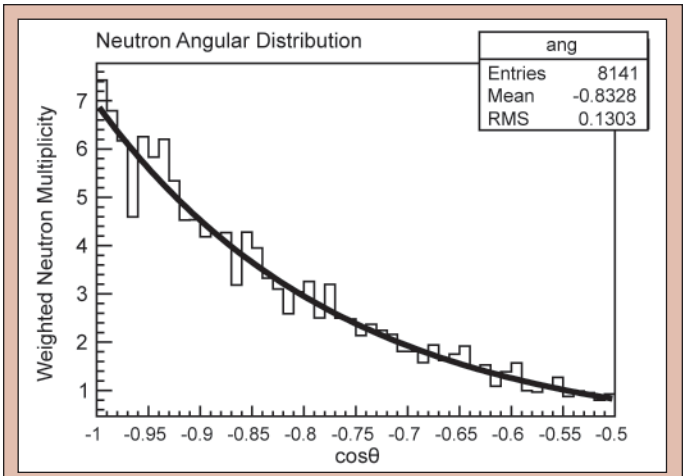

Figure 3. The neutron angular distribution at A-A' in Figure 2. The neutron fluence can be treated as isotropic in each bin [10]. The fluence was scored at z = 0 m with a 2 m radius scoring plane with the assumption of the isotropy in the first bin ($-1 < \cos\theta < -0.99$).

			Neutron total 'weight'		Neutron total number	
Run Number	**Type of Bias**	**Computation Time**	**At z = 300 m**	**At z = 0**	**At z = 300 m**	**At z = 0**
1	No biasing	23 hours 35 min	82	2	82	2
2	Leading particle biasing activated for EMF particles (for e-,e+ < 2.5 GeV and γ < 2.5 GeV)	1 hour 36 min	103	0	87	0
3	Decay length biasing activated for photonuclear interactions (biasing factor = 0.020)	6 hours 46 min	103	0.781	5008	49
4	Splitting in waterdump activated for photons (10 regions in waterdump, factor of 2 for each region boundary)	6 hours 22 min	96.4	1.09	16619	117

Table 1. Computation time and effectiveness of each bias. All runs were made with 6,000 electrons incident on the water dump and each run contains the biases of all previous runs.

This was a consequence of the relatively small number of incident electrons that were simulated compared to the large rates of incident electrons expected at the ILC and did not accurately reflect the IP fluence. To obtain better statistics, a circular scoring plane 2 m in radius at z = 0 was used. Due to the isotropic fluence assumption, the fluence calculated with this scoring plane, per square centimeter, was assumed to be the same as that measured with a 1.5 cm radius circle after a sufficiently long time.

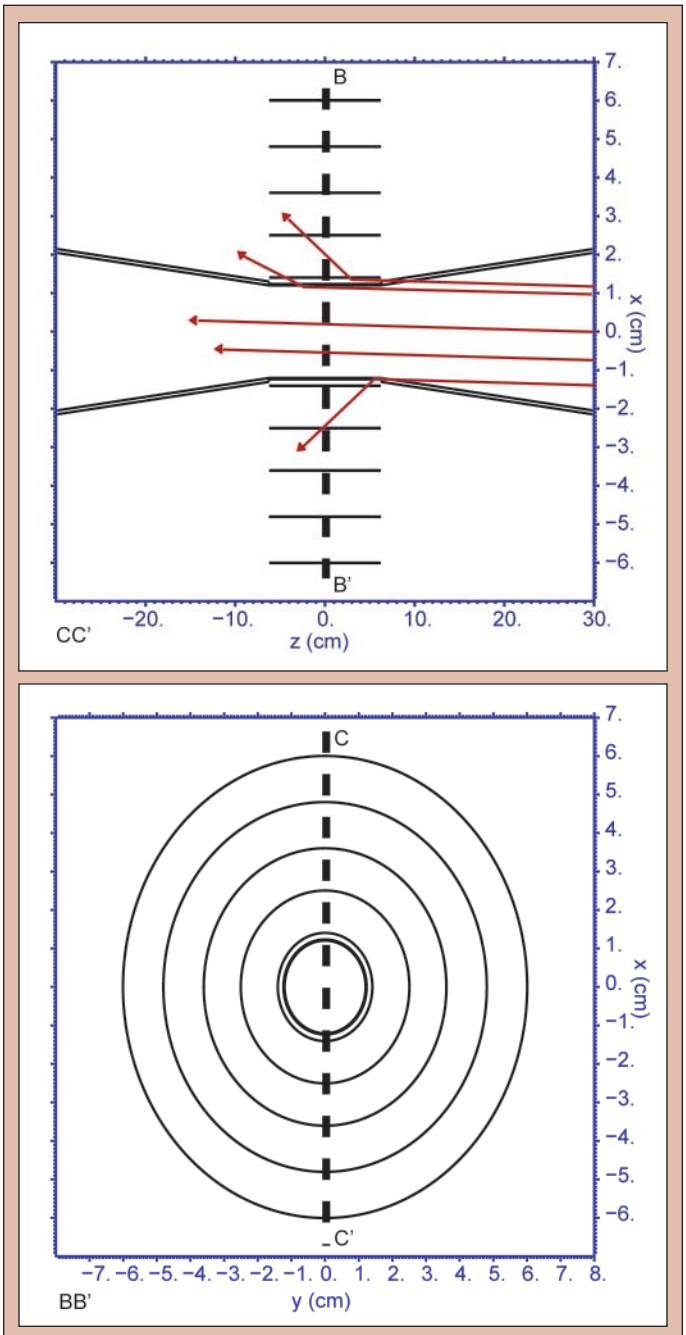

Figure 4. The CCD silicon vertex detector in the SiD detector model. The five layers of the detector were modeled by concentric cylinders, each 0.01 cm thick. The beampipe barrel was made 0.04 cm thick and the conical section was made 0.1 cm thick. The left and right conical sections of the beampipe extend outward to -167.9 cm and +167.9 cm respectively, but have been truncated here at -30 cm and +30 cm [11].

As a primary benchmark estimate, 10^4 electrons were collided into the water dump and the IP fluence was measured with no material in the beamline. A concrete collimator and a concrete tunnel wall were then added to the simulation, as shown in Figure 2. The number of incident electrons was increased to $5x10^4$ to overcome the anticipated drop in statistics from the addition of the collimator, and the IP fluence was measured again. Finally, the tunnel was removed, the collimator was kept in place, and the IP fluence was measured with $5x10^4$ incident electrons to study neutrons which scatter off of the tunnel walls and towards the detector.

Once the IP fluence was determined, the neutron fluence from the quadrupole QDEX1 to the five layers of the CCD silicon vertex detector, the detector fluence, was studied, since the neutrons that reach the IP do not necessarily collide with the detector elements. The central barrel beryllium beampipe and the five layers of the Si barrel vertex detector were placed around the IP, as shown in Figure 4, and were based on the geometry specified at the Snowmass conference [11]. Figure 5 shows the full model of the detector and the nearest section of the extraction line, which consists of QDEX1

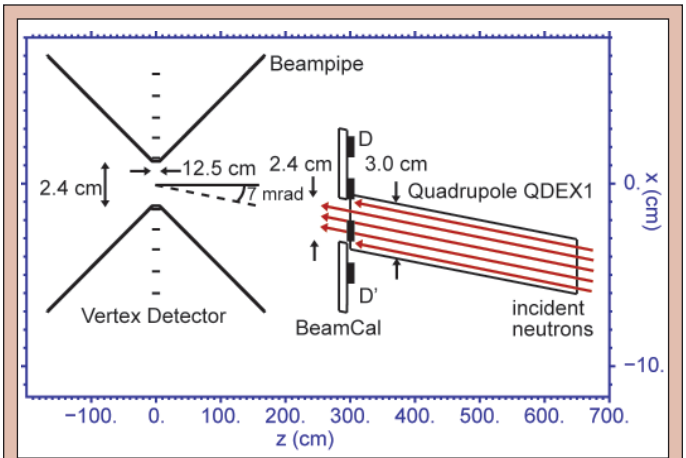

Figure 5. The full model of the extraction line. The BeamCal was modeled by a 12.5 cm thick slab of tungsten. The neutron source was evenly distribution on the surface of the quadrupole at D-D' and the neutrons were given a trajectory of 7 mrad towards the detector.

and the BeamCal. The BeamCal was modeled by a 12.5 cm thick slab of tungsten; the Si layers in it were ignored since they have a low probability of scattering the incident neutrons.

The neutron energy and 'weight' distributions at A-A' in Figure 2 were recorded from the previous simulations and were sampled from and used to generate a neutron source. Figure 6 shows the energy distribution. The initial positions of the neutrons in the source were generated randomly in the bore of QDEX1 at D-D' in Figure 5 in a circle of 1.5 cm radius centered at x = -2.1 cm and y = 0 cm. This starting point modeled the neutrons from the water dump that would reach the surface of the quadrupole from the dump without being blocked by collimators, magnets, or other material. All neutrons in the source were given a 7 mrad trajectory from the z-axis.

The detector fluence was measured and combined with the IP fluence when the tunnel and collimator were in place, to provide an estimate of the total fluence at the vertex detector. The total

fluence values were converted to annual fluxes to obtain a temporal picture of the neutron displacement damage. The measurement was performed twice more, when the BeamCal was removed and when it was replaced with an infinitely absorbing material, in order to give an estimate of the BeamCal scattering. The BeamCal was then returned and the flux as a function of the BeamCal aperture radius was studied.

Finally, a normalized and comparable value was obtained for the amount of damage done to the first layer of the vertex detector by neutron backshine. Previous research has studied the amount of displacement damage done to CCD silicon detectors by neutrons as a function of neutron energy and has produced a 1 MeV equivalent silicon displacement damage scale (see Figure 7) [12]. The total fluence in the first silicon layer was scaled according to this distribution. Although the neutron energy distribution in Figure 6 extends beyond the upper bound of the experimental data, which occurs at $2x10^7$ eV, the data reaches a plateau above 10^7 eV, and this trend was used to scale the neutrons above 0.01 GeV. The calculated fluence would underestimate the damage if highly energetic neutrons require a higher scaling factor than this, though it does at least provide a lower bound. In addition, the calculated fluence provides an upper bound on the fluences in the other layers and, as such, they were left unscaled, but would also have a greater scaled flux due to their similar input neutron energy distributions.

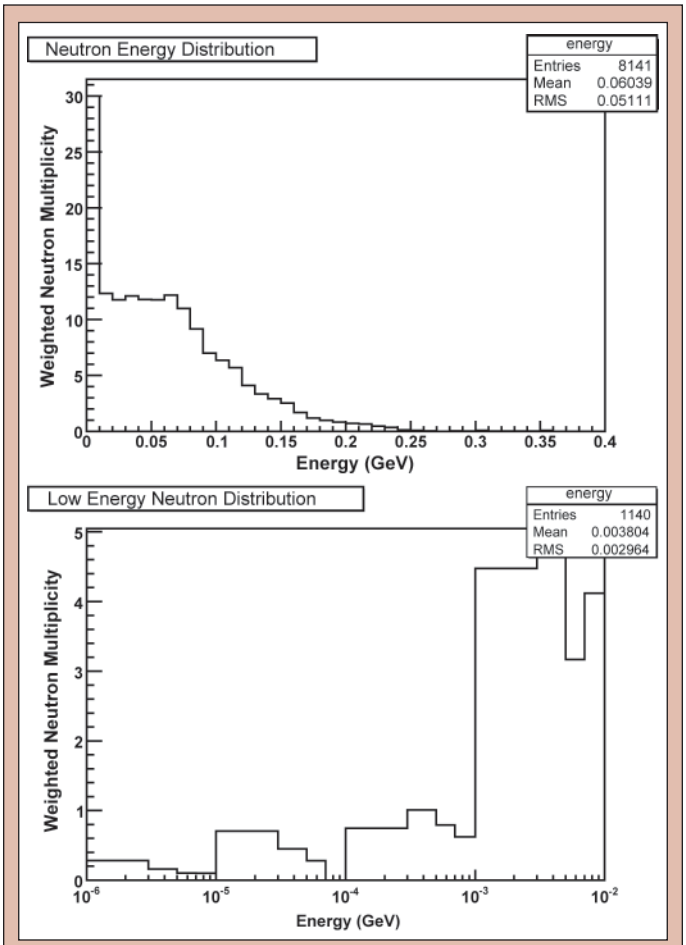

Figure 6. a) The neutron energy distribution collected at A-A' in Figure 2. b) The low energy neutron distribution for neutrons in the first bin in Figure 6a.

Results

The IP flux with no objects in the extraction line was measured to be $8.3x10^{10}$ +/- $1.5x10^{10}$ neutrons/cm^2/year. When the tunnel and collimator were added for a more accurate estimate, the flux dropped to $3.7x10^{10}$ +/- $2.3x10^{10}$ neutrons/cm^2/year. When the tunnel was removed, there was no appreciable change in the flux given the current level of statistics, as it remained at $3.7x10^{10}$ +/- $3.3x10^{10}$ neutrons/cm^2/year. The computation time and effectiveness of the biasing techniques used in the IP flux scoring are shown in Table 1.

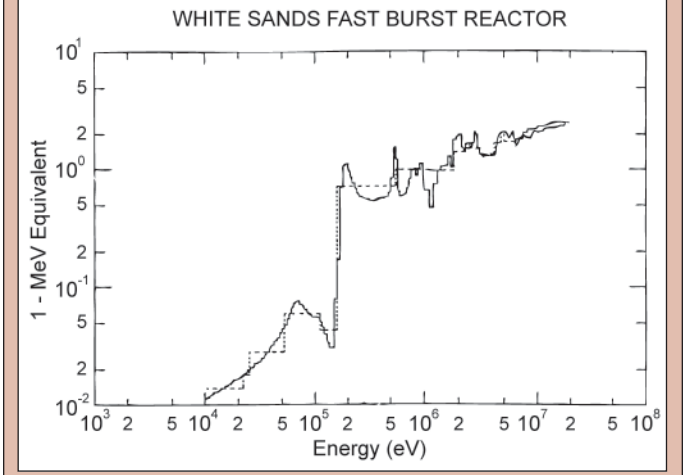

Figure 7. Silicon displacement as a function of energy. The neutron energy distribution in Figure 6 extends beyond the upper bound of this experimental data. The data was approximated to remain constant at the $2*10^7$ eV value above this energy level. Figure was made by T. M. Flanders and M. H. Sparks [12].

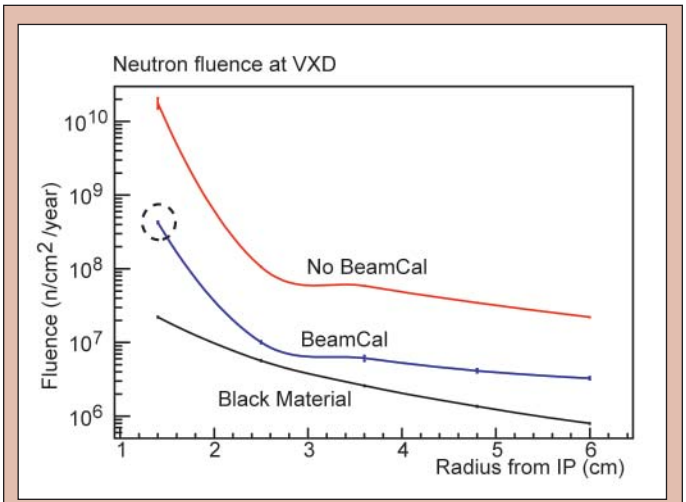

Figure 8. The fluence as a function of radius from the IP for three modifications of the BeamCal. The circled value, $4.28*10^8$ neutrons/cm^2/year, is of particular importance, since it corresponds to the current BeamCal type and aperture radius.

Figure 8 shows the fluence at the five layers of the inner detector for the three different modifications of the BeamCal. For the first layer, there was over an order of magnitude difference between the cases when there was a BeamCal and when there was no BeamCal, the former having a fluence of 4.3×10^8 neutrons/cm^2/year and latter having one of 1.8×10^{10} neutrons/cm^2/year. There was a larger difference between the cases when there was a BeamCal and there was black absorbing material, the latter having a fluence of 2.2×10^7 neutrons/cm^2/year. In all three cases, the fluence in layers two to five dropped far below that in layer 1. The neutron fluence of 4.3×10^8 neutrons/cm^2/year at the first layer when the BeamCal was in place is of particular importance, since it was found for the present status of the extraction line, and is shown circled in Figure 8. This neutron fluence at the detector is 1.2% of the fluence that reaches the IP, with the rest of the neutrons passing through the empty space in the detector or scattering off the Be beampipe harmlessly (see Figure 4).

The energy distribution of the neutrons that contribute to this fluence shows a large number of neutrons with energy greater than 10 MeV, implying that the current nominal fluence underestimates the displacement damage power (see Figure 9). This distribution, corrected with the information from Figure 8, gives the 1 MeV damage equivalent neutron fluence to be 9.3×10^8 neutrons/cm^2/year, which is a factor of two larger than the unscaled value.

The symmetric positron beam contributes the same amount of displacement damage, meaning the final corrected fluence is 1.9×10^9 neutrons/cm^2/year. In one year, this amounts to 19% of the 10^{10} neutrons/cm^2 flux that would degrade the vertex detector to the point of repair or replacement.

Figure 10 shows the fluence at the five layers of the detector as the BeamCal aperture was expanded; the fluence increases as the aperture is opened.

Discussion and Conclusions

The neutron fluence at the IP when there is no material in the extraction line, which was 8.3×10^{10} +/- 1.5×10^{10} neutrons/cm^2/year, is the highest level of background that is possible at the detector from backscattering from the beam dump if one assumes that every particle that reaches the IP will damage the vertex detector. The collimator in front of the dump blocked roughly half of this flux, since the fluence decreased by a factor of two to 3.7×10^{10} +/- 3.3×10^{10} neutrons/cm^2/year when the collimator was added. There was no appreciable increase in fluence when the tunnel was added given the current level of statistics, as it remained at 3.7×10^{10} +/- 2.3×10^{10} neutrons/cm^2/year. This should not be interpreted to mean that there is no scattering off the tunnel walls, as the root-mean-square (RMS) deviation in the fluences once the collimator was added was more than 50% of the fluence itself. The amount of scattering is an important value to know when looking for potential solutions to reduce the backscattering problem. One solution being considered is to move the water dump out of a direct line of sight from the detector and to place a dipole immediately before the collimator to bend the trajectory of the beam towards the dump. If neutrons do not scatter off the tunnel walls, this would be an effective solution. However, if the neutrons do scatter off the tunnel walls and act like a gas of particles moving back towards the detector, as suspected, then bending the beam would not reduce this background source. A further study of neutron scattering is being conducted.

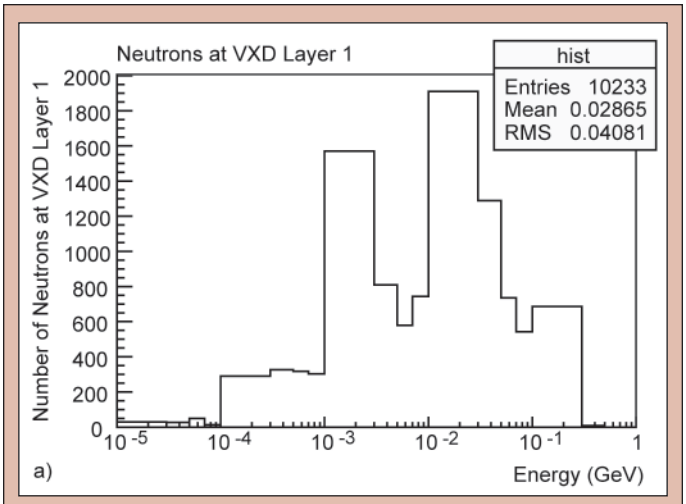

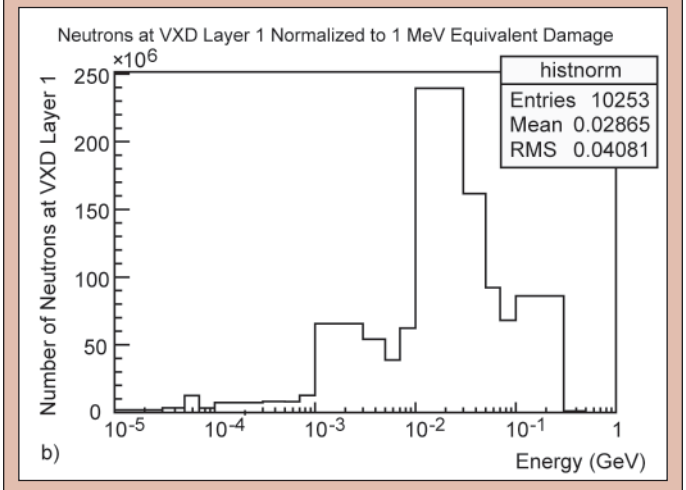

Figure 9. a) The neutron energy distribution for the flux that reaches the first layer of the silicon detector. b) The neutron energy distribution scaled to 1 MeV equivalent neutron displacement damage to CCD silicon detectors.

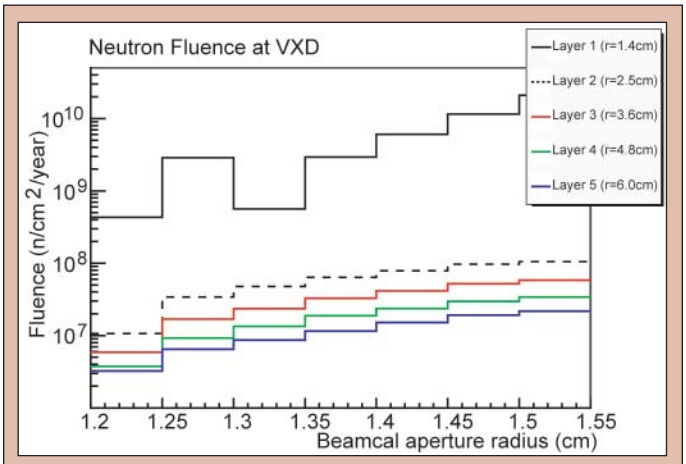

Figure 10. The neutron fluence at the five layers of the vertex detector as the aperture radius of the BeamCal is expanded. At a radius of 1.5 cm, the BeamCal blocks none of the incident neutrons.

The computation time and effectiveness of the biasing techniques for 6,000 incident electrons are shown in Table 1. As columns 6 and 7 show, statistics increased by a factor of 203 at the surface of the dump and by a factor of 59 at the IP. This allowed the estimation of a more stable IP fluence and provided a large distribution from which to sample in order to produce the neutron source. The total 'weight' of the neutrons recorded at z = 300 m and z = 0 m, shown in columns 4 and 5, was preserved as the different biases were applied, meaning that the biases did not obscure the underlying physics when improving the statistics. This validated the use of these biases with 10^4 and $5x10^4$ incident electrons when estimating the IP fluence.

The sharp drop in the fluence at layer 1 of the vertex detector from $1.8x10^{10}$ to $4.3x10^8$ neutrons/cm^2/year, shown in Figure 8, implies that the BeamCal acts like a collimator and impedes the flow of neutrons through it by 97%. Since this large amount of collimation is not the intent of the BeamCal, the effect of the fluence on its tungsten and silicon layers are being studied in further detail. When the black absorbing material is in place, there is no direct line of sight from the quadrupole bore to the detector, and the only neutrons that can hit the detector are those that scatter off of the beryllium beampipe. Thus, the further drop in the fluence, to $2.2x10^7$ neutrons/cm^2/year, for the case of the black absorbing material gives the estimate that 5.2% of the neutrons that hit the detector have scattered off of the beampipe, and the rest have hit it along their direct line of sight. Furthermore, the order of magnitude drop in the fluence between layer 1 and layers 2 to 5 of the silicon detector show that the outer layers are well shielded from the neutron fluence and are not a concern; attention should be focused on the innermost layer which takes the bulk of the displacement damage. The endcap sections of the silicon detector are being added and their effect on the fluence at all of the layers is being studied.

The neutron energy at the vertex detector is more heavily distributed above 10 MeV, as shown in Figure 9, which implies that the damage to the detector is greater than the nominal fluence. The corrected 1 MeV equivalent neutron fluence of $9.3x10^8$ neutrons/cm^2/year is properly normalized and can be compared to the threshold value of 10^{10} neutrons/cm^2. When the positron beam is considered and the fluence doubles to $1.9x10^9$ neutrons/cm^2/year, the neutron backscattering from the dump contributes 19% of the threshold value in one year. Even if this were the only background, the detector would degrade within 6 years; a longer lifetime is desired.

Although the current background level is not overwhelming, the relationship in Figure 10 is an important consideration when analyzing the effect of other neutron backgrounds in the detector. Two particularly important neutron backgrounds arise from electron-positron pairs produced from beam-beam interactions and synchrotron radiation produced from the quadrupoles used to focus the beams immediately before the IP; both products can hit the BeamCal and produce neutrons through electromagnetic showers [13]. This is the dominant source of neutron background, as the neutrons produced at the BeamCal are located near the vertex detector and cannot be shielded. A simple method to reduce this flux would be to open the BeamCal aperture to prevent interactions. However, as Figure 10 shows, a tradeoff exists, since doing so would increase the neutron background from the extraction line beam dump. In the extreme case, the BeamCal could be opened up larger than the extraction line quadrupole aperture, and the dump background would equal $2.1x10^{10}$ neutrons/cm^2/year, which would require the vertex detector to be replaced every six months.

These results have directed further studies towards the main sources of neutron backgrounds, including electron-positron pairs, Bremstrahlung photons, and radiative Bhabha scattering, in order to obtain a complete picture of the overall neutron damage done to the vertex detector and to understand the tradeoffs that exist in attempting to suppress it. The detector model will also be improved and the effect of the neutron flux on the endcap tracking chambers and other elements will be studied. The neutron damage in the CCD silicon detector must be minimized in order to ensure detector longevity as well as minimal repairs of the detector components, allowing the ILC to effectively perform measurements and discover new fundamental physics.

Acknowledgements

This research was conducted at the Stanford Linear Accelerator Center, located in Menlo Park, California, USA. I would like to thank the Department of Energy for giving me with the opportunity to participate in the SULI program. Most importantly, I would like to thank my two supervisors, Dr. Takashi Maruyama and Dr. Lewis Keller, whose knowledge, enthusiasm, and dedication made the work and the experience both exciting and rewarding. I would also like to acknowledge Mario Santana for his help resolving problems with FLUKA and Dr. Nan Phinney for presenting me with this research opportunity. Finally, I would like to thank Dr. Tom Markiewicz and Nicholas Arias for their generous help throughout the summer.

References

[1] ATLAS Collaboration, "ATLAS Detector and Physics Performance Technical Design Report," ATLAS TDR 14, CERN/LHCC 99–14, Vol. 1, pp. 3, 25 May 1999.

[2] G. Aarons *et al.*, "International Linear Collider Reference Design Report," ILC Global Design Effort and World Wide Study, Vol. 3: Accelerator, pp. 2.1-1 to 2.1-5, August 2007.

[3] G. Aarons *et al.*, "International Linear Collider Reference Design Report," ILC Global Design Effort and World Wide Study, Vol. 3: Accelerator, pp. 2.7-1 to 2.7-18, August 2007.

[4] R. B. Neal Editor, "The Stanford Two-Mile Accelerator," pp. 706–709, 1968.

[5] W. R. Dawes, Jr., "Overview of Radiation Hardening for Semiconductor Detectors," *Nuclear Instruments and Methods in Physics Research*, A 288, pp. 54–61, 1990.

[6] J. E. Brau and N. Sinev, "Operation of a CCD Particle Detector in the Presence of Bulk Neutron Damage,"

IEEE Transactions on Nuclear Science, vol. 47, no. 6, pp. 1898–1901, December 2000.

[7] The FLUKA team, *Online FLUKA manual*, INFN and CERN, version 2006.3b, March 2007.

[8] G. Lindstrom, "Radiation damage in silicon detectors," *Nuclear Instruments and Methods in Physics Research*, A 512, pp. 30–43, 2003.

[9] A. Chilingarov, J. S. Meyer, and T. Sloan, "Radiation damage due to NIEL in GaAs particle detectors," Nuclear Instruments and Methods in Physics Research, A 395, pp. 35–44, 1997.

[10] R. B. Neal Editor, "The Stanford Two-Mile Accelerator," pp. 1035–1040, 1968.

[11] N. Graf, SLAC Confluence, sidaug05, July 23, 2005, http://confluence.slac.stanford.edu/display/ilc/sidaug05

[12] T. M. Flanders and M. H. Sparks, "Monte Carlo calculations of the neutron environment produced by the White Sands Missile Range Fast Burst Reactor," *Nuclear Science and Engineering*, vol. 103, pp. 265–275, 1989.

[13] T. Abe *et al*., "SiD Detector Outline Document," pp. 30, 19 May 2006.